Figure S1

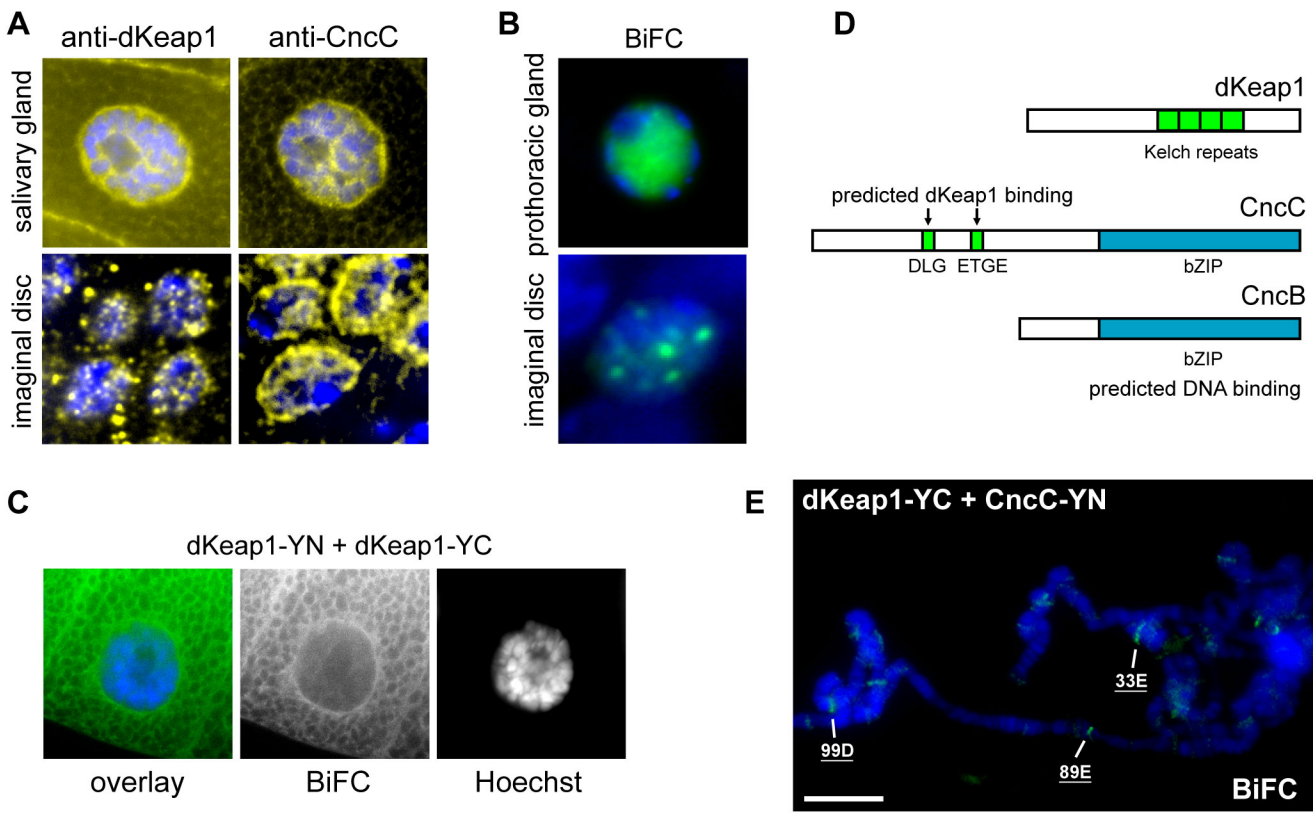
A
anti-dKeap1
anti-CncC
salivary gland
imaginal disc
B
BiFC
prothoracic gland
imaginal disc
D
dKeap1
Kelch repeats
predicted dKeap1 binding
CncC
DLG ETGE
bZIP
CncB
bZIP
predicted DNA binding
C
dKeap1-YN + dKeap1-YC
overlay
BiFC
Hoechst
E
dKeap1-YC + CncC-YN
33E
99D
89E
BiFC

Figure S1. Subcellular localization of endogenous dKeap1 and CncC as well as of dKeap1-CncC BiFC complexes in different tissues

(A) Subcellular localization of endogenous dKeap1 and CncC in salivary gland and imaginal disc cells. Salivary glands and wing imaginal discs from wild-type 3rd instar larvae were stained using antibodies raised against dKeap1 and CncC. The immunofluorescence (yellow) was superimposed on Hoechst fluorescence (blue).
Interpretation: Endogenous dKeap1 and CncC are predominantly nuclear in *Drosophila* tissues, consistent with the nuclear localization of ectopic dKeap1 and CncC in living cells (see Fig. 1A).

(B) Visualization of dKeap1-CncC BiFC complexes in prothoracic gland and imaginal disc cells. The intrinsic BiFC fluorescence was visualized in the prothoracic gland and in the wing imaginal disc from 3rd instar larvae that expressed the dKeap1 and CncC BiFC fusions indicated under the control of the *5015-GAL4* and *71B-GAL4* drivers, respectively. The *5015-GAL4* driver activates transcription in prothoracic glands and in salivary glands (Yoshiyama et al., 2006). The *71B-GAL4* driver activates transcription in imaginal discs and in salivary glands (Busson and Pret, 2007). The BiFC fluorescence (green) was superimposed on Hoechst fluorescence (blue).
Interpretation: The dKeap1-CncC BiFC complexes were present within the nuclei of polyploid prothoracic gland cells and diploid imaginal disc cells. Thus, dKeap1-CncC BiFC complexes were localized to the nuclei in different tissues and cell types (also see Fig. 1A).

(C) Visualization of dKeap1-dKeap1 BiFC complexes in salivary gland cells. The intrinsic BiFC fluorescence was visualized in salivary glands from 3rd instar larvae that expressed the dKeap1 BiFC fusions indicated under the control of the *Sgs3-GAL4* driver (Cherbas et al., 2003). The BiFC (green) and Hoechst fluorescence (blue) were superimposed and shown separately.
Interpretation: dKeap1 homodimers are localized almost exclusively to the cytoplasm, in contrast to the predominantly nuclear localization of dKeap1-CncC complexes as well as of endogenous dKeap1 and CncC (see Fig 1A and supplementary material Fig. S1A,B).

(D). Diagrams of dKeap1, CncC and CncB. Regions that are conserved between CncC and mammalian Nrf2 are shown in color. Regions that are predicted to mediate dKeap1-CncC interaction are shown in green.

(E) Visualization of loci that are bound by dKeap1-CncC BiFC complexes on polytene chromosomes in larvae reared at higher temperature. Intrinsic BiFC fluorescence was visualized on polytene chromosome spreads from larvae that expressed dKeap1-YC and CncC-YN. The larvae were reared at 29°C.
Interpretation: dKeap1 and CncC BiFC complexes bound the same loci in larvae that were reared at 29°C as in larvae that were reared at 21°C (Fig. 1B). The detailed conditions of fusion protein expression therefore did not influence the loci that were bound by the BiFC complexes.

Figure S2

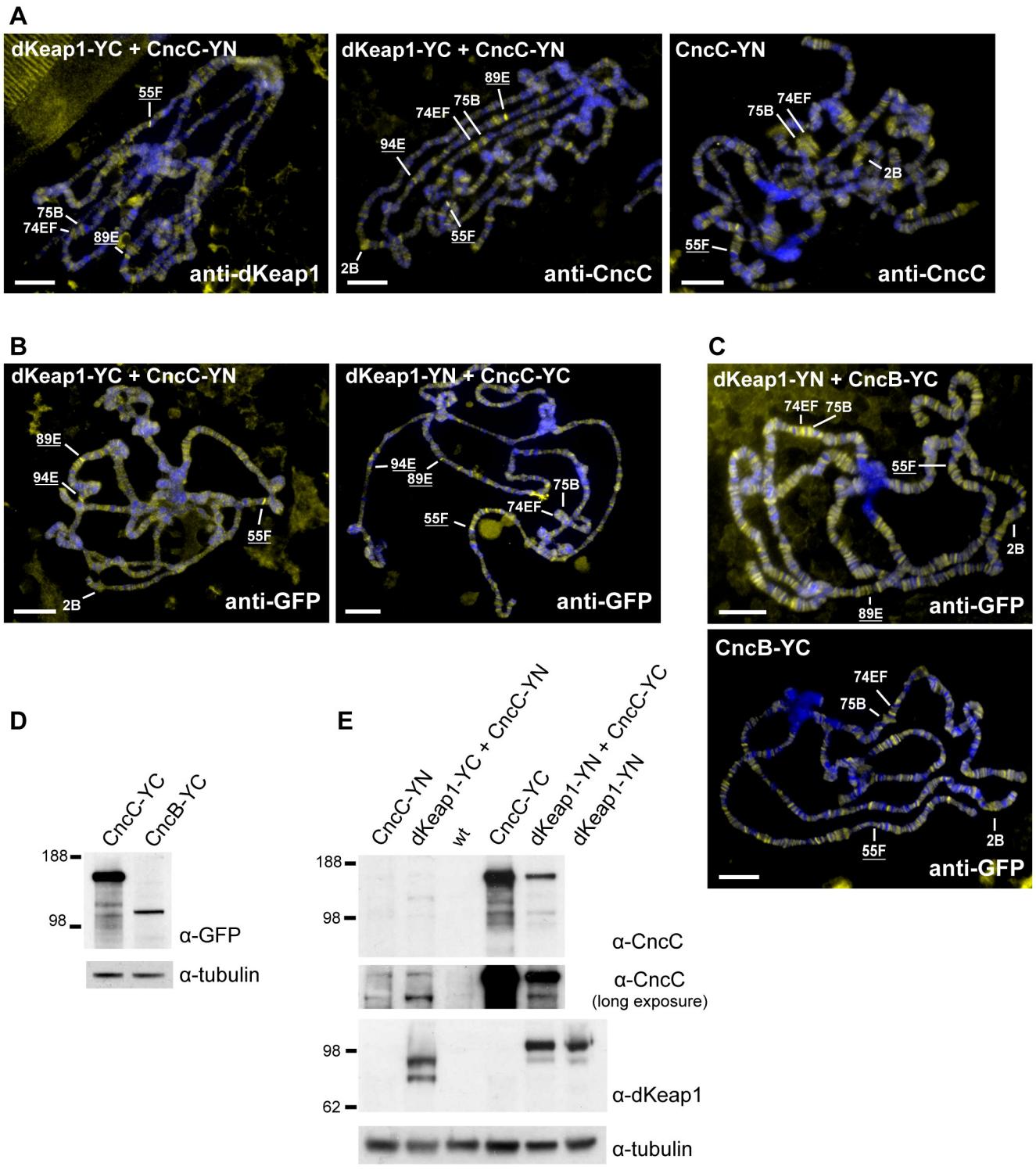
A
dKeap1-YC + CncC-YN
55F
75B
74EF
89E
anti-dKeap1
dKeap1-YC + CncC-YN
89E
75B
74EF
94E
55F
2B
anti-CncC
CncC-YN
74EF
75B
2B
55F
anti-CncC
B
dKeap1-YC + CncC-YN
89E
94E
55F
2B
anti-GFP
dKeap1-YN + CncC-YC
94E
89E
75B
74EF
55F
anti-GFP
C
dKeap1-YN + CncB-YC
74EF 75B
55F
2B
89E
anti-GFP
CncB-YC
74EF
75B
55F
2B
anti-GFP
D
CncC-YC
CncB-YC
188
98
α-GFP
α-tubulin
E
CncC-YN
dKeap1-YC + CncC-YN
wt
CncC-YC
dKeap1-YN + CncC-YC
dKeap1-YN
188
98
α-CncC
α-CncC
(long exposure)
98
62
α-dKeap1
α-tubulin

Figure S2. Differences between the loci occupied by dKeap1 and CncC and their expression levels when they were co-expressed or expressed separately

(A) Loci occupied by dKeap1-YC and CncC-YN when they were co-expressed versus expressed separately. Polytene chromosome spreads were prepared from larvae that expressed the fusion proteins indicated at the top of each panel in salivary glands under the control of the *Sgs3-GAL4* driver. The loci that were occupied by the fusion proteins were visualized by immunostaining using the antibodies indicated at the bottom of each panel. Immunofluorescence (yellow) was superimposed on Hoechst fluorescence (blue). The loci that were occupied by co-expressed CncC and dKeap1 (55F and 89E), as well as the ecdysone regulated puffs that were occupied by CncC and dKeap1 expressed separately (2B, 74EF, and 75B) are indicated on those polytene chromosome spreads where they could be mapped. The scale bars are 10 μm.
Interpretation: dKeap1 and CncC bound to distinct loci when they were co-expressed *versus* expressed separately. The same difference in binding was observed when different combinations of dKeap1 and CncC fusion proteins were expressed (dKeap1-YC + CncC-YN or dKeap1-YN + CncC-YC) (compare with Fig. 2A).

(B) Detection of the loci occupied by co-expressed dKeap1 and CncC fusion proteins on polytene chromosomes by immunostaining using anti-GFP antibodies. Polytene chromosome spreads from larvae that expressed the fusion proteins indicated at the top of each panel in salivary glands under the control of the *Sgs3-GAL4* driver were stained with antibodies against GFP.
Interpretation: The shift in binding upon dKeap1 and CncC co-expression was detected using antibodies directed against CncC, dKeap1 as well as GFP (compare with Fig. 2A,C).

(C) Loci occupied by dKeap1 and CncB when they were co-expressed and by CncB when it was expressed separately. Polytene chromosome spreads from larvae that expressed the fusion proteins indicated at the top of each panel in salivary glands under the control of the *Sgs3-GAL4* driver were stained using antibodies directed against GFP. Immunofluorescence (yellow) was superimposed on Hoechst fluorescence (blue).
Interpretation: CncB-YC occupied numerous loci that overlapped with the loci occupied by CncC-YC and CncC-YN, including 55F, 89E, 2B, 75B and 74EF (compare with Fig. 2A and S2A). Nevertheless, the CncB and CncC fusions did not occupy identical loci. Co-expression of dKeap1 and CncB fusions did not enhance their binding at the 55F and 89E loci in contrast to the co-expression of dKeap1 and CncC. Therefore, the change in binding produced by dKeap1 and CncC co-expression required direct interaction between the proteins.

(D) Comparison of the levels of CncC and CncB fusion proteins. Extracts from the salivary glands of larvae that carried the transgenes indicated above the lanes under the control of the *Sgs3-GAL4* driver were analyzed by immunoblotting using anti-GFP and anti-tubulin antibodies as indicated to the right of the blots.

Interpretation: The level of CncB-YC expression was lower than that of CncC-YC and higher than that of CncC-YN (see supplementary material Fig. S2E).

(E) Comparison of the levels of CncC and dKeap1 fusion proteins expressed separately and in combination. Extracts from control salivary glands and from salivary glands that carried the transgenes indicated abovethe lanes under the control of the *Sgs3-GAL4* driver were analyzed by immunoblotting using anti-CncC, anti-dKeap1 and anti-tubulin antibodies as indicated to the right of the blots.
Interpretation: The levels of expression of the CncC fusion proteins (CncC-YN *versus* CncC-YC) differed more than 10-fold. Nevertheless, co-expression of each of the CncC fusions with dKeap1 fusions (dKeap1-YN + CncC-YC and dKeap1-YC + CncC-YN) shifted the loci that were occupied by the CncC fusion proteins regardless of their levels of expression (see Fig. 2A, supplementary material Fig. S2A). Endogenous CncC was barely detectable, indicating that the levels of expression of the CncC fusion proteins were much higher than that of endogenous CncC.

Figure S3

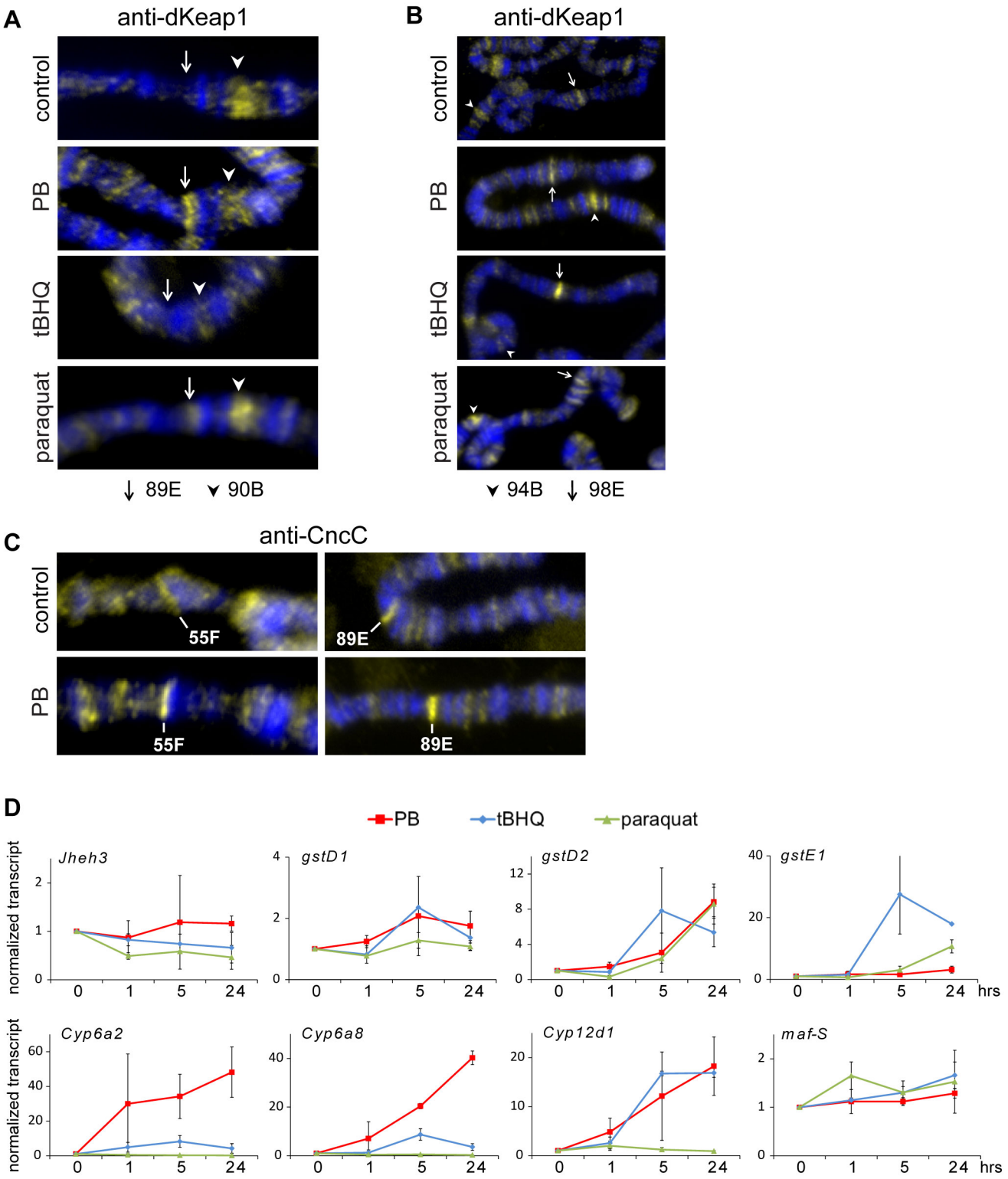
A
anti-dKeap1
control
PB
tBHQ
paraquat
89E
90B
B
anti-dKeap1
control
PB
tBHQ
paraquat
94B
98E
C
anti-CncC
control
PB
55F
89E
55F
89E
D
PB
tBHQ
paraquat
normalized transcript
Jheh3
gstD1
gstD2
gstE1
Cyp6a2
Cyp6a8
Cyp12d1
maf-S
0
1
5
24
hrs

Figure S3. Effects of phenobarbital and other xenobiotic compounds on CncC occupancy and on xenobiotic response gene transcription

(A) Effects of phenobarbital, tBHQ, and paraquat feeding to larvae on dKeap1 binding at the 89E locus. Polytene chromosomes from 3rd instar larvae that were fed phenobarbital (PB), tBHQ, paraquat or control food for 24 hours were stained using anti-dKeap1 antibodies. Segments of polytene chromosomes containing the 89E (arrows) and 90B (arrowheads) loci are shown.
Interpretation: Phenobarbital feeding increased endogenous dKeap1 binding at the 89E locus relative to the level of dKeap1 binding at the adjacent 90B locus. dKeap1 binding at the 89E locus in control larvae and in larvae that were fed tBHQ or paraquat was not detectable.

(B) Effects of phenobarbital, tBHQ, and paraquat feeding to larvae on dKeap1 binding at the 98E locus. Polytene chromosomes from 3rd instar larvae that were fed phenobarbital (PB), tBHQ, paraquat or control food for 24 hours were stained using anti-dKeap1 antibodies. Segments of polytene chromosomes containing the 98E (arrows) and 94B (arrowheads) loci are shown.
Interpretation: tBHQ feeding, but not phenobarbital or paraquat feeding, increased endogenous dKeap1 binding at the 98E locus relative to the level of dKeap1 binding at the adjacent 94B locus. The lack of dKeap1 binding at the 55F and 89E loci in these larvae was therefore not due to a failure of tBHQ feeding to influence dKeap1 binding.

(C) Effects of phenobarbital feeding on ectopic CncC occupancy at the 55F and 89E loci. Larvae that expressed CncC-YN in salivary glands under the control of the *Sgs3-GAL4* driver were fed phenobarbital (PB) or control food for 24 hours. Polytene chromosome spreads from these larvae were stained with antibodies against CncC.
Interpretation: Phenobarbital feeding increased ectopically expressed CncC binding at the 55F and 89E loci. No endogenous CncC binding was detected at the 55F or the 89E locus in control larvae or in larvae that were fed phenobarbital. The failure to detect endogenous CncC binding was potentially due to the higher level of background staining of polytene chromosomes by anti-CncC antibodies.

(D) Effects of phenobarbital, tBHQ, and paraquat on xenobiotic response gene transcription at different times after feeding. The transcripts indicated above the graphs were measured in 3rd instar larvae that were fed phenobarbital (PB, red lines), tBHQ (blue lines), paraquat (green lines) for 1, 5, or 24 hours. The levels of the transcripts indicated were normalized by the levels of the transcripts in larvae that were fed control food. The transcript levels were normalized by the levels of *Rp49* transcripts. The data shown represent the means and standard deviations from two separate experiments.
Interpretation: Phenobarbital, tBHQ, and paraquat feeding selectively activated the transcription of different genes at different times (compare with Fig. 3E).

Figure S4

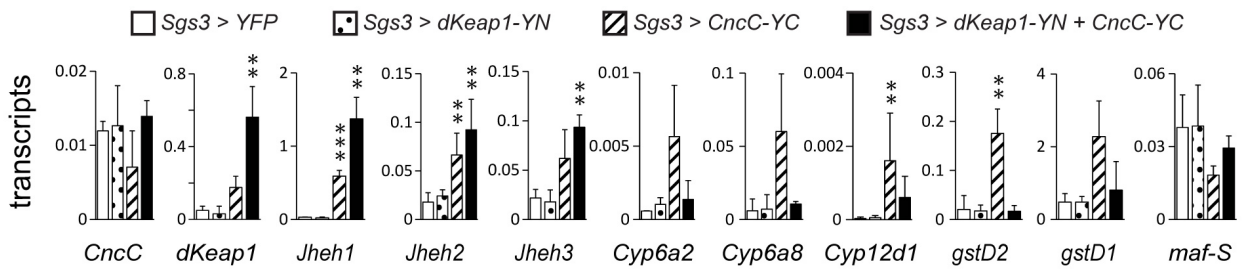

Figure S4. Effects of ectopic dKeap1 and CncC expression on transcription of genes that are bound by dKeap1-CncC complexes and on that of other xenobiotic response genes

Comparison of the effects of dKeap1 and CncC BiFC fusion proteins expressed separately and in combination on transcription of different genes. The levels of the transcripts indicated below the bar graphs were measured in the salivary glands of 3rd instar larvae. The transcripts were isolated from 10 pairs of salivary glands for each condition. All transcript levels were normalized by the levels of *Rp49* transcripts and correspond to the means and standard deviations from two separate experiments. The significance of the differences in transcription in transgenic *versus* control larvae was evaluated using ANOVA (**, $p<0.05$; ***, $p<0.01$).
Interpretation: The co-expression of ectopic dKeap1 and CncC fusion proteins synergistically activated transcription of the *Jheh* and *dKeap1* genes. In contrast, the co-expression of ectopic dKeap1 with CncC suppressed the activation of other xenobiotic response genes by CncC. The co-expression of different combinations of dKeap1 and CncC fusion proteins had consistently opposite effects on the transcription of these genes (also see Fig. 5B).

Figure S5

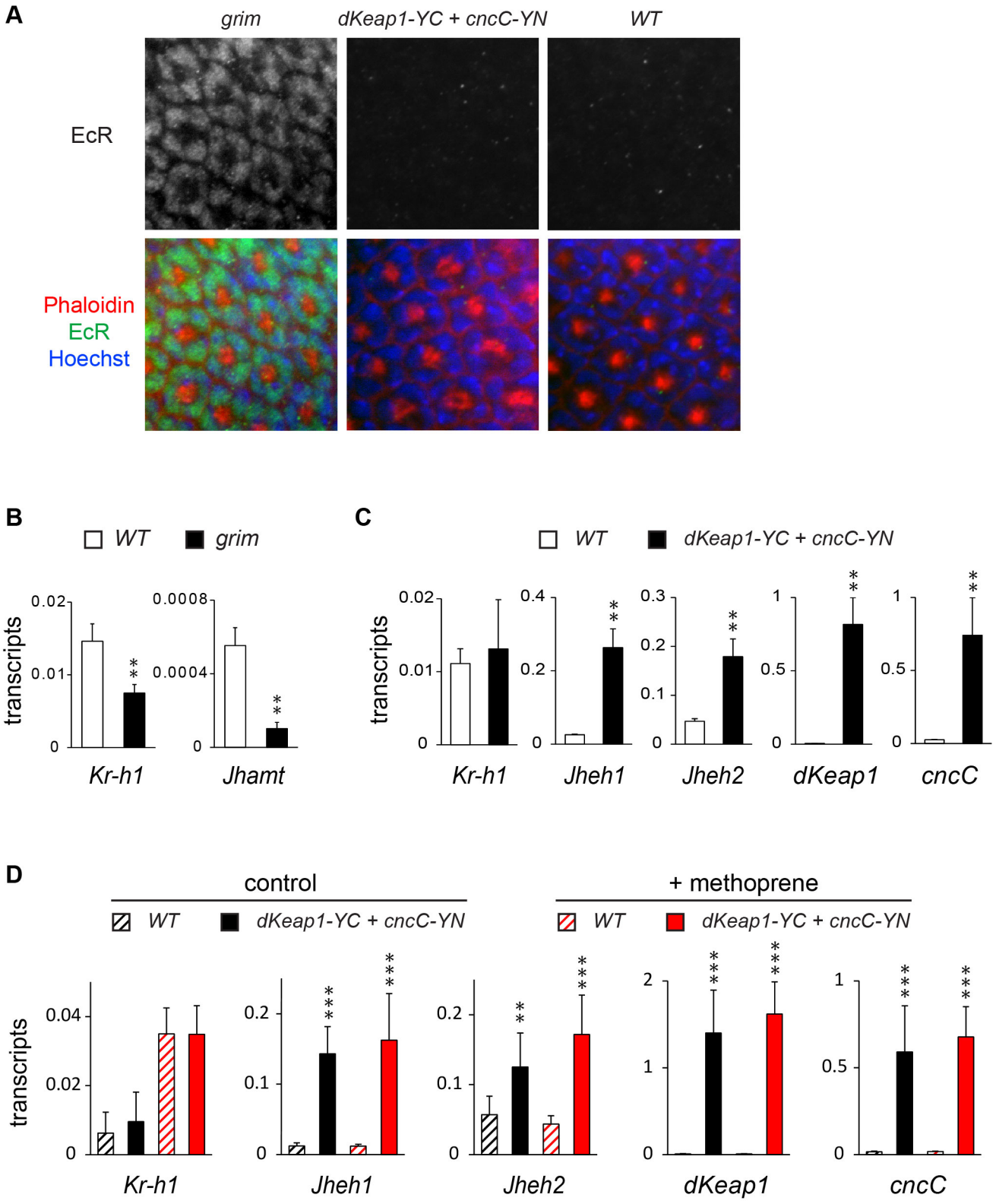
A
grim
dKeap1-YC + cncC-YN
WT
EcR
Phaloidin
EcR
Hoechst
B
WT
grim
transcripts
0.02
0.01
0
0.0008
0.0004
0
Kr-h1
Jhamt
C
WT
dKeap1-YC + cncC-YN
transcripts
Kr-h1
Jheh1
Jheh2
dKeap1
cncC
D
control
+ methoprene
WT
dKeap1-YC + cncC-YN
transcripts
0.04
0.02
0
0.2
0.1
Kr-h1
Jheh1
Jheh2
2
1
0.5
dKeap1
cncC

Figure S5. Ectopic dKeap1 and CncC co-expression does not alter juvenile hormone-dependent functions

(A) Effects of dKeap1 and CncC co-expression, and of corpora allata ablation on the timing of ecdysone receptor expression in the optic disc. Eye discs were isolated from pupae 2 hours after the pre-white pupae stage and immunolabeled as described (Phalle Bde, 2004). Ecdysone receptor (EcR) expression was compared between pupae that expressed *grim* under the control of the *Aug21-GAL4* driver (Mirth et al., 2005), pupae that co-expressed dKeap1 and CncC under the control of the *tubulin-GAL4 driver* and the temperature sensitive $GAL80^{ts}$ repressor (McGuire et al., 2004), and control pupae (WT). To inactive $GAL80^{ts}$, 3rd instar larvae were transferred from 19°C to 29°C 36 hours after molting. The developing ommatidia were counterstained using phalloidin. The EcR immunofluorescence (green), phalloidin (red) and Hoechst (blue) images were superimposed.
Interpretation: Ablation of the corpora allata by grim expression induced premature ecdysone receptor expression in the optic disc as shown previously (Riddiford et al., 2010). No ecdysone receptor expression was observed at this stage in control pupae or in pupae that co-expressed dKeap1 and CncC. dKeap1 and CncC co-expression and corpora allata ablation had distinct effects on EcR expression in the eye disc.

(B) Effects of corpora allata ablation on Kr-h1 expression in the 3rd instar larvae. The levels of the transcripts indicated above the graphs were measured in 3rd instar larvae that expressed *grim* under the control of the *Aug21-GAL4* driver (grim) and control larvae (WT), and were normalized by the levels of *Rp49* transcripts. The data shown represent the means and standard deviations from two separate experiments. The significance of the differences in the transcript levels between grim transgenic and control pupae was determined by using ANOVA (**, $p<0.05$).
Interpretation: *Jhamt* is a juvenile hormone biosynthetic gene that is specifically expressed in the corpora allata. The decrease in *Jhamt* transcription is consistent with ablation of the corpora allata by grim expression. The decrease in the level of *Kr-h1* transcripts upon corpora allata ablation suggests that juvenile hormone enhances *Kr-h1* transcription in 3rd instar larvae.

(C) Effects of dKeap1-CncC co-expression on Jheh and Kr-h1 transcription. The levels of the transcripts indicated below the bar graphs were measured in 3rd instar larvae that co-expressed dKeap1 and CncC under the control of the *Tubulin-GAL4* driver and the temperature-sensitive $GAL80^{ts}$ repressor (solid bars) as well as in control larvae (open bars). Larvae were collected 24 hours after transferring them from 19°C to 29°C to inactivate $GAL80^{ts}$. All transcript levels were normalized by the levels of *Rp49* transcripts. The data shown represent the means and standard deviations from two separate experiments. The significance of the differences in transcript levels between transgenic and control larvae was evaluated by ANOVA (***, $p<0.01$).
Interpretation: The levels of *Jheh1* and *Jheh2* transcripts were induced by conditional dKeap1 and CncC fusion protein co-expression. No change in *Kr-h1* transcripts was detected in these larvae.

(D) Effects of methoprene administration and dKeap1-CncC co-expression on Jheh and Kr-h1 transcription. 3rd instar larvae that co-expressed dKeap1 and CncC under the control of the *Tubulin-GAL4* driver and the temperature-sensitive *GAL80^{ts}* repressor (solid bars) as well as the control larvae (striped bars) were transferred from 19°C to 29°C 36 hours after molting. White pre-pupae derived from these larvae were treated with 0.2 µl of 0.3% methoprene, a juvenile hormone mimic, in acetone (red bars) or acetone alone (black bars). The levels of the transcripts indicated below the graphs were measured in pupae 24 hours after pupation, and were normalized by the levels of *Rp49* transcripts. The data shown represent the means and standard deviations from five separate experiments. The significance of the differences in transcript levels between transgenic and control pupae were tested by ANOVA (**, $p<0.05$; ***, $p<0.01$).
Interpretation: The level of *Kr-h1* transcripts was increased by methoprene. It was not affected by dKeap1 and CncC co-expression in pupae, whereas *Jheh1* and *Jheh2* transcripts were induced.

Supplementary Materials and Methods

Plasmid expression vectors

The dKeap1-YN and CncC-YN expression vectors encoded residues 1-173 of YFP fused to the C-termini of dKeap1 and CncC, respectively, in pUAST (Brand and Perrimon, 1993). The dKeap1-YC, CncC-YC and CncB-YC expression vectors encoded residues 174-238 of YFP fused to the C-termini of dKeap1, CncC and CncB, respectively, in pUAST. The YFP-dKeap1 and YFP-CncC expression vectors encoded rxYFP fused to the N-termini of dKeap1 and CncC, respectively, in pUAST. rxYFP contains the N149C and S202C substitutions in YFP (Ostergaard et al., 2001).

BiFC analysis of protein interactions on polytene chromosomes

Salivary glands that expressed BiFC fusion proteins were isolated from early wandering 3rd instar larvae that were reared at 21°C to enhance the polyploidy of salivary gland cells (Johansen et al., 2009). Polytene chromosome spreads were prepared using an acid-free squash technique to avoid quenching of the BiFC fluorescence (Johansen et al., 2009). One pair of salivary glands was dissected in PBS and then incubated in freshly prepared 2% paraformaldehyde in Brower's Fixation Buffer (0.15 M PIPES, 3 mM $MgSO_4$, 1.5 mM EGTA, 1.5% NP40, pH6.9) for 3 minutes, in PBST (PBS + 0.2% Triton X-100) for 3 minutes, and in 50% glycerol allowing to soak for 5 minutes. The salivary glands were then transferred to 10 µl of 50% glycerol, and squashed between a coverslip coated with Sigmacote (Sigma) and a microscope slide coated with poly-lysine (Sigma). The slides were frozen in liquid nitrogen and the coverslips were removed using a razor blade immediately after taking them from the liquid nitrogen. The slides were incubated in PBS for 15 min followed by staining with Hoechst 33258 (Molecular Probes) in PBS for 10 minutes. The preparations were then washed with PBS for 5 minutes, dried, and mounted in 80% glycerol containing 10 mM Tris pH 9.0. All images were acquired on Olympus IX81 inverted fluorescence microscope with a Hamamatsu ORCA-ER digital CCD camera. BiFC signal was visualized using 504 nm excitation and 542 nm emission wavelengths. The signals corresponding to each combination of excitation and emission wavelengths were pseudocolored and merged in RGB color space.

Antisera, conventional polytene chromosome squash, immunostaining and imaging

Anti-dKeap1 and anti-CncC antisera were raised against proteins encompassing residues 620-776 of dKeap1 and residues 88-344 of CncC fused to GST. The antisera were affinity purified by incubating them with Nitrocellulose membranes with dKeap1 or CncC fusion proteins, followed by elution.

Polytene chromosome squashes were prepared by dissecting 2-3 pairs of salivary glands and fixing them in freshly prepared 200 µl PBS + 4% paraformaldehyde + 1% Triton X-100 for 1 minute followed by incubation in freshly prepared 200 µl 45% acetic acid + 4% paraformaldehyde for 2 minutes. The fixed salivary glands were transferred to 10 µl 16.7% lactoacetic acid + 25% acetic acid and squashed between a coverslip coated with Sigmacote (Sigma) and a microscope slide coated with poly-lysine (Sigma) as described in detail in Johansen et al. (2009). The polytene

chromosome squashes were immuno-labeled as described (Johansen et al., 2009; Silver and Elgin, 1976).

Immuno-labeling of whole salivary glands, the brain complexes (including prothoracic gland), and imaginal discs from 3rd instar larvae and of brain complexes (including eye disc) from 2 hour pupae were performed as described (Phalle Bde, 2004). Antibodies were diluted as follows: anti-GFP (Fitzgerald Industries Intl.) (1:200), anti-dKeap1 (1:100), anti-CncC (1:100), anti-EcR (Ag10.2, Developmental Studies Hybridoma Bank) (1:200), Alexa Fluor 594 conjugated goat anti-rabbit (Invitrogen) (1:1000). To stain F-actin, pupal brain complexes were incubated in 0.2 U/µl Rhodamine phalloidin (Molecular Probes) in PBST + 1% BSA for 20 minutes. The samples were mounted in VectaShield (Vector Laboratories). For live imaging, tissues were dissected, mounted in PBS and imaged within 5 minutes after dissection. rxYFP signal was visualized using 504 nm excitation and 542 nm emission wavelengths. Rhodamine phalloidin signal was visualized using 540 nm excitation and 565 nm emission wavelengths.

Immunoblotting

Four 3rd instar larvae were homogenized in 50 µl ice-cold Buffer (20 mM Tris-HCl pH8.0, 0.2% NP-40, 0.2% Triton X-100, 150 mM NaCl, 5 mM EDTA, 1 mM EGTA, 2 mM $NaVO_3$, protease inhibitor cocktail (Roche) and 1 mM PMSF). The samples were resolved using a NuPAGE 4-12% Bis-Tris gel (Invitrogen). The proteins were transferred to Nitrocellulose membrane (Bio-Rad) and probed using dKeap1 antiserum (1:500), CncC antiserum (1:500) or anti-α-tubulin antibody (12G10, Developmental Studies Hybridoma Bank) (1:500). HRP-conjugated secondary antibodies (GE healthcare UK limited) were used to detect immune complexes.

Transcript quantitation

Four 3rd instar larvae or 10 pairs of salivary glands dissected from early wandering 3rd instar larvae in PBS prepared using DEPC water were used for mRNA extraction by the RNeasy kit (Qiagen) following the protocol. Isolated mRNA was treated with RQ1 RNase-Free DNase (Promega) and reverse transcribed using the Transcriptor First Strand cDNA Synthesis Kit (Roche). Real-time qPCR was performed using SYBR Green I Master (Roche) in a LightCycler 480 II (Roche). The relative transcript levels were calculated by assuming that they were proportional to 2^{-Cp}, and were normalized by the levels of *Rp49* transcripts. Primer sequences were designed using Universal ProbeLibrary software (Roche) and are listed in supplementary material Table S1.

Statistical analyses

The significance of the differences in the relative transcript levels measured by RT-qPCR were evaluated using one-way ANOVA.

Table S1. Primer sequences used to measure the transcript levels by RT-qPCR

gene	5'-primer	3'-primer
Rp49	CGGATCGATATGCTAAGCTGT	GCGCTTGTTCGATCCGTA
cncC	GAGGTGGAAATCGGAGATGA	CTGCTTGTAGAGCACCTCAGC
dKeap1	CAAGGAGTCGGAGATGTCG	GTAGAGGATGCGTGACATGG
Jheh1	TCACTTCACCACCGATATTCAG	CTTTGTTGTCATCATAAACCATCAG
Jheh2	TCCTACCCTTCGACATCAGC	GACGACTCAGCTGACCGATT
Jheh3	ACCTGACCAAGTGGGATGAG	TCGGATACCTTTTCGTGGAT
Cyp6a2	GCGCAACGAGATCCAAAC	TGTAGAGCCTCAGGGTTTCTG
Cyp6a8	CAAGATAAGGTTCGGGCTGA	TGGTGTACAGTCGCAGAGTTTC
Cyp12d1	TGTTTGACTGATGAAATGCAGAT	AGCGAGGTTTGCACAACAAT
gstD1	TCGCGAGTTTCACAACAGAA	TGAGCAGCTTCTTGTTCAGC
gstD2	CGGACATTGCCATCCTGT	TGCTGAAGTCGAACTCACTAACTT
gstE1	GGACTACGAGTACAAGGAGGTGA	TCACATATTCCTCGCTCAGGT
maf-S	CCGGAGAACCTTAAAGAATCG	TCTCCAGCTCGTCCTTCTGT
Kr-h1	GAATTCTCCGGACTTTATAGAACAA	GCTGGTTGGCGGAATAGTAA
Jhamt	TTGACCATGTCACCTCGTTC	TCCGAGAGCTCCTTTCAGAT

Supplementary References

Brand, A.H., and Perrimon, N. (1993). Targeted gene expression as a means of altering cell fates and generating dominant phenotypes. *Development* **118**, 401-415.

Busson, D., and Pret, A.M. (2007). GAL4/UAS targeted gene expression for studying Drosophila Hedgehog signaling. *Methods Mol Biol* **397**, 161-201.

Cherbas, L., Hu, X., Zhimulev, I., Belyaeva, E., and Cherbas, P. (2003). EcR isoforms in Drosophila: testing tissue-specific requirements by targeted blockade and rescue. *Development* **130**, 271-284.

Johansen, K.M., Cai, W., Deng, H., Bao, X., Zhang, W., Girton, J., and Johansen, J. (2009). Polytene chromosome squash methods for studying transcription and epigenetic chromatin modification in Drosophila using antibodies. *Methods* **48**, 387-397.

McGuire, S.E., Mao, Z., and Davis, R.L. (2004). Spatiotemporal gene expression targeting with the TARGET and gene-switch systems in Drosophila. *Sci STKE 2004*, pl6.

Mirth, C., Truman, J.W., and Riddiford, L.M. (2005). The role of the prothoracic gland in determining critical weight for metamorphosis in Drosophila melanogaster. *Curr Biol* **15**, 1796-1807.

Ostergaard, H., Henriksen, A., Hansen, F.G., and Winther, J.R. (2001). Shedding light on disulfide bond formation: engineering a redox switch in green fluorescent protein. *EMBO J* **20**, 5853-5862.

Phalle Bde, S. (2004). Immunostaining of whole-mount imaginal discs. *Methods Mol Biol* **247**, 373-387.

Riddiford, L.M., Truman, J.W., Mirth, C.K., and Shen, Y.C. (2010). A role for juvenile hormone in the prepupal development of Drosophila melanogaster. *Development* **137**, 1117-1126.

Silver, L.M., and Elgin, S.C. (1976). A method for determination of the in situ distribution of chromosomal proteins. *Proc Natl Acad Sci U S A* **73**, 423-427.

Yoshiyama, T., Namiki, T., Mita, K., Kataoka, H., and Niwa, R. (2006). Neverland is an evolutionally conserved Rieske-domain protein that is essential for ecdysone synthesis and insect growth. *Development* **133**, 2565-2574.